ACS Catalysis

pubs.acs.org/acscatalysis Letter

Structure-Guided Tuning of a Hydroxynitrile Lyase to Accept Rigid Pharmaco Aldehydes

Yu-Cong Zheng, Fu-Long Li, Zuming Lin, Guo-Qiang Lin, Ran Hong,* Hui-Lei Yu,* and Jian-He Xu*

Cite This: *ACS Catal.* 2020, 10, 5757−5763 Read Online

ABSTRACT: The chiral vicinal C−O/C−N bifunctional groups generated from enzymatic hydrocyanation represents a useful methodology. However, construction of the pharmacophore of β_2-adrenoreceptor agonists with this method remains a great challenge because of complete racemization of the benzylic alcohol during deprotection of the acetal groups. In this study, structure-guided redesign of a hydroxynitrile lyase originating from *Prunus communis* (*Pc*HNL5) enables a highly enantioselective hydrocyanation of rigid benzo-ketal aldehyde which was proved to be resistant against racemization during the deprotection step, with dramatically improved productivity (>95% conversion vs <1%). X-ray structure analysis and kinetic study revealed the side chain of L331 tunes the substrate adaptability of bulky and rigid benzo-ketal aldehyde, thereby facilitating the formation of a series of valuable unnatural cyanohydrins in high enantiopurities and good yields. Furthermore, the HNL variant L331A was successfully applied for a gram-scale chemo-enzymatic synthesis of (*R*)-Salmeterol, a long-term β_2-adrenoreceptor agonist, in an optically pure form (>99% ee) with an overall yield of 54%, which is the highest value reported.

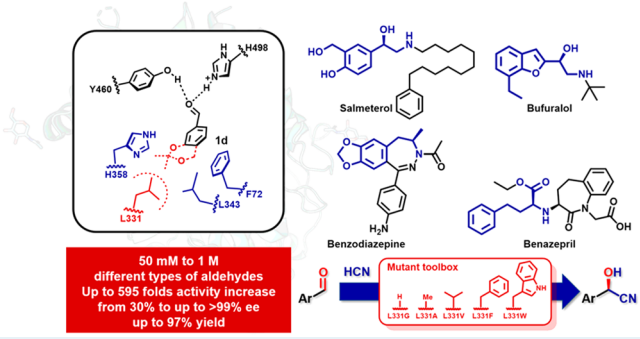

KEYWORDS: *cyanohydrin, hydrocyanation, hydroxynitrile lyase, protein engineering, β_2-adrenoreceptor agonist*

Enantioselective C−C bond formation is of the utmost importance in organic synthesis.[1] Despite the development of numerous chemical methods,[2] enzymatic C−C bond formation has emerged as a greener process and an attractive complementary approach that often affords high enantioselectivity.[3] Currently, lyases (e.g., EC 4.1.x.x) are used for enzymatic C−C bond formation,[3a,4] among which only hydroxynitrile lyase (HNL) catalyzes both C−C and C−X (X = O or N) bond formation in hydrocyanation or nitro-aldol reactions.[5] The vicinal C−O or C−O/C−N functional groups generated from the method provide an indispensable tool in the construction of key structural motifs with pharmaceutical significance.[6] Distinct from purely chemical systems, synthetic methodologies involving HNLs usually suffer from inherent conflicts between the harsh synthetic requirements and a limited availability of suitable biocatalysts, except a few famous examples through protein engineering.[7] In addition, spontaneous nonselective HCN addtion/cyanohydrin racemization happens when pH > 4.5, thus ideal enzymatic hydrocyanations prefer to be performed under a very acidic environment, which raises challenges for both the stability and activity of the enzyme.[5a,b] In general, HNLs have been reported to be highly specific toward simple aldehydes (like benzaldehyde or flexible chain aldehydes); however, further development of this classical biocatalytic tool remains a great challenge toward sterically rigid aldehyde substrates in spite of their highly synthetic values. We noticed a series of β_2-adrenergic receptor agonists are used widely to treat asthma and other pulmonary disorders.[8] Formation of the common 1,2-amino alcohol moiety of classical β_2-adrenergic receptor agonists (e.g., salmeterol, salbutamol, vilanterol, and salmefamol) (Scheme 1) has attracted several innovative chemical or biochemical transformations. These methods involve chemical[9] or microbial reduction of ketones,[10] metal-[11] or chiral auxiliary[12] mediated hydrogen transfer, oxy-Michael addition of an nitro-olefin,[13] and the Henry reaction.[14] However, these approaches generally required multistep syntheses of designated substances and/or high loading of sophisticated catalysts. An early example of enzymatic hydrocyanation of the 1,3-oxane ring fused benzaldehydes **1b** and **1c** applied in the synthesis of salbutamol failed because of complete racemization and partial decomposition of the product during the final acetal-deprotection step.[15] The easy removal of the isopropylidene moiety without appreciable racemization[16] of the benzylic

Received: March 6, 2020
Revised: April 19, 2020
Published: April 28, 2020

https://dx.doi.org/10.1021/acscatal.0c01103
ACS Catal. 2020, 10, 5757−5763

Scheme 1. Strategy to Redesign a Biocatalyst to Facilitate Enantioselective Hydrocyanation of Pharmaceutically Demanding but Sterically Rigid Aldehydes[a]

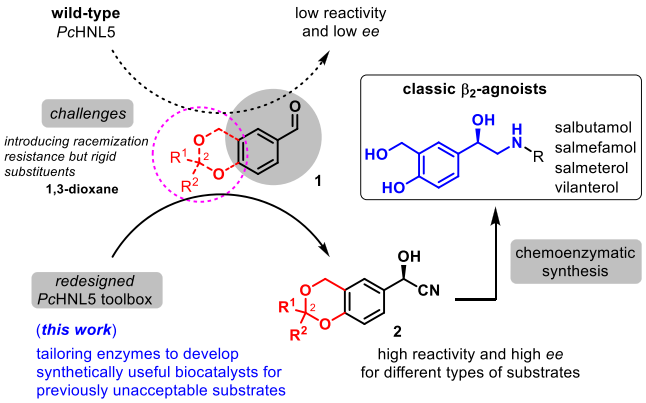

[a] **1a**, benzaldehyde, highlighted in gray; **1b**, $R^1 = R^2 = H$; **1c**, $R^1 = H$ or Me, R^2 = Me or H; **1d**, $R^1 = R^2 = Me$.

alcohol encouraged us to execute asymmetric hydrocyanation of 2,2-dimethyl-4*H*-benzo[*d*][1,3]dioxine-6-carbaldehyde (**1d**) by using *Pc*HNL5 (from *Prunus communis*), which was recently identified in our lab, with a good activity and high stability under an acid environment (Figure S3).[17]

Although *Pc*HNL5 exhibited a broad substrate tolerance for many substituted benzaldehydes assayed, a dramatic decrease in hydrocyanation activity was observed when a rigid 1,3-dioxane ring was introduced with further decreases for substrates bearing extra methyl groups on the methylene site. For example, *Pc*HNL5 showed the highest activity toward its natural substrate, benzaldehyde (**1a**) (85 U mg^{-1} protein), whereas the activity for aldehyde **1b** bearing a 1,3-dioxane ring was moderate (1.5 U mg^{-1} protein). The enzyme activity toward aldehyde **1d** proved to be extremely sluggish with the activity decreasing to less than 0.005% when compared with that of **1a**. Moreover, the optical purity of the enzyme-catalyzed cyanohydrin product **2d** was poor because the enzymatic activity could not override the competing non-enzymatic HCN addition to the aldehyde during the reaction.

This extremely low reactivity of *Pc*HNL5 toward bulky substrate **1d** motivated us to undertake the redesign of the HNL structure through protein engineering which has emerged as a powerful tool in tailoring the enzyme for desired properties.[18] We recently determined the crystal structures of deglycosylated *Pc*HNL5 (PDB ID 6JBY) as well as the enzyme in complex with **1a** (PDB ID 6JQY) and its corresponding cyanohydrin (*R*)-**2a** (PDB ID 7BWP). The geometry of the active pocket of wild-type (WT) *Pc*HNL5 comprises a winding substrate tunnel and a deeply buried, but relatively large, hydrophobic pocket (Figure S120). Similar to other FAD-dependent HNLs,[19] the FAD in *Pc*HNL5 does not directly participate in proton transfer, instead the cyanohydrin cleavage/formation proceeds via the general acid/base catalysis through residue His498 (Figure S122). The substrate pose is stabilized by hydrogen bonding of the substrate carbonyl group with His498 and Tyr460, while the aromatic ring is stabilized in the large hydrophobic pocket (Figure 1A). Because of the essential position of Phe72, Leu331, Leu343, and His358 in the substrate tunnel as revealed by Caver 3.0[20] as well as their presumed roles in accommodating the dioxane ring and the hydrophobic ketal group, these four residues were chosen for

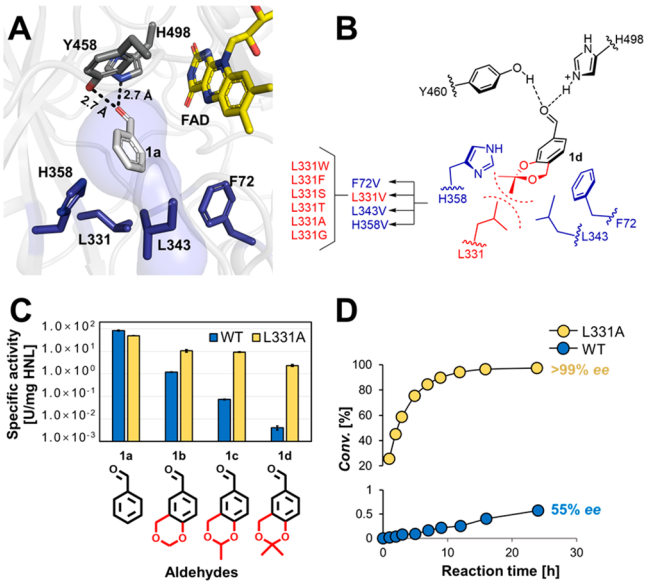

Figure 1. (A) Structural insights into the binding pose of substrates **1a** in the active pocket of crystal complex of wild-type *Pc*HNL5 with **1a** (PDB ID 6LQY). The key interactions of the substrate carbonyl group with residues His498 and Tyr458 or the positions chosen for mutation (B) are indicated. (B) The candidate residues that might affect the reactivity of substrate **1d** in the *Pc*HNL5 active pocket. The pale blue shadow represents substrate access calculated by the Caver 3.0 algorithm. Residues surrounding substrate access are shown as dark blue stick models. Impact of the L331 mutation on substrate specificity toward bulky benzaldehyde derivates. (C) Asymmetric hydrocyanation activity of wild-type (WT) *Pc*HNL5 (blue) and its variant L331A (yellow) toward substrates **1a**−**1d**. (D) The performance of the *Pc*HNL5 variant L331A versus WT for hydrocyanation of **1d** (1 mL of biphasic reaction mixture was composed of 0.2 mg of purified HNL, 0.3 mL of citrate buffer (100 mM, pH 3.5), 0.7 mL of HCN-MTBE (2 M), and 0.2 mmol of **1d**).

valine scanning (i.e., the four targeted residues were replaced by the relatively smaller and moderately hydrophobic valine to explore if steric hindrance or hydrophobicity will affect the activity significantly).[21]

Pronounced increases were observed with all of the residues considered (Table S5). The most substantial increases in specific activity toward **1d** were achieved upon mutation of Leu331. Thus, this residue was further replaced by six preselected amino acids (Trp, Phe, Thr, Ser, Ala, and Gly) to reshape the entrance to the substrate pocket by varying the extent of steric hindrance and the degree of hydrophobicity (Figure 1B). The single site mutant L331A showed remarkable enhancements in activity toward 1,3-oxane ring-fused benzaldehydes (Figure 1C). In particular, the activity of variant L331A toward **1d** (2.4 U mg^{-1} protein) was 545-fold higher than that of the WT *Pc*HNL5. These results encouraged us to evaluate the catalytic performance of structurally tailored *Pc*HNL5 in hydrocyanation reactions, with a biphasic system containing 200 mM **1d** and an equal amount of the purified enzyme (Figure 1D). For variant L331A, the reaction was completed in 16 h, and product **2d** was yielded with 96% conversion and >99.8% ee. In contrast, only a trace conversion (<1%) and a low optical purity (55% ee) of the product were obtained with WT *Pc*HNL5, even if the reaction time was prolonged to 24 h.

To understand how the mutagenesis causes a significant increase of enzyme activity, the crystal structure of L331A was

https://dx.doi.org/10.1021/acscatal.0c01103
ACS Catal. 2020, 10, 5757−5763

solved (PDB ID 6LR8). Further insights were obtained by docking simulation of **1d** with the wild type and the mutant crystal structures since attempts to obtain the crystal complexes with **1d** were unsuccessful. A distinct difference in the substrate binding pose was observed (Figure 2): replacing

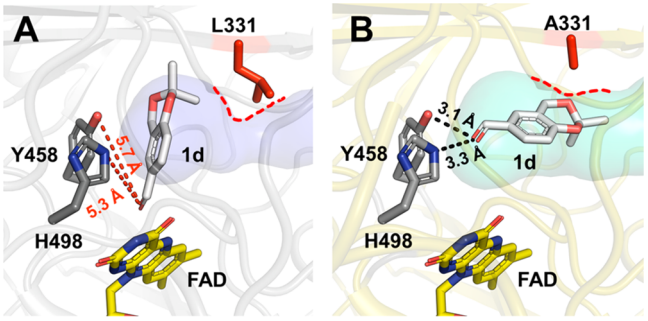

Figure 2. Docking simulations of **1d** with *Pc*HNL5 wild-type (A) and L331A mutant (B). Side chain of position 331 is presented as a red stick, with the dashed line highlighting the contact with the substrate tunnel. Shadow represents the substrate tunnels of the WT enzyme (pale blue) and L331A (pale green).

of the side chain of Leu331 into alanine leads to a dramatically enlarged substrate tunnel and an extra space for accommodation of the rigid dioxane ring and two methyl groups. Besides, the attacking distances between the aldehyde group of **1d** and residues His498 and Tyr460 in L331A become much shorter (~3 Å vs >5 Å) than the wild type, due to a 99.3° deflection of the benzo-ring plane (Figure S120) from the original hard-to-attack conformation, indicating that a sufficiently strong hydrogen bonding network with **1d** is successfully rebuilt by mutation for facilitating the hydrocyanation reaction.

We subsequently determined the saturation kinetic constants of WT *Pc*HNL5 and several representative variants (L331A, L331V, L331G) with substrates **1a**−**1d** (Table 1). Substitution of Leu331 to the smaller-sized hydrophobic residue alanine caused a remarkable decrease in K_m (from 36 to 2.2 mM) and a large increase in turnover rate (k_{cat} from 2.6 × 10^{-2} to 4.1 s^{-1}) for substrate **1d**. However, further reduction in size by mutation to glycine did not affect the affinity with **1d** (i.e., no further decrease in K_m beyond that of L331A). Instead, variant L331G showed a clear decrease in k_{cat} from 4.1 to 1.4 s^{-1}, which is consistent with the initially assayed specific activities (Table S5). The best variant for **1d** (L331A) also exerts strong activity toward **1c**, with a 297-fold higher catalytic efficiency (k_{cat}/K_m) than the WT enzyme. However, for aldehyde **1b** (with a relatively smaller substituent), the best Leu331 variant was L331 V, with the lowest K_m (6.9 mM) observed. Moreover, larger K_m values were observed toward substrate **1a** when Leu331 was replaced by smaller side chain amino acids Val, Ala, and Gly. Because Leu331 is located at the bottleneck of the substrate tunnel, these results suggest that the side chain shape and/or size of residue 331 can regulate the substrate adaption of the enzyme for bulky aryl aldehydes.

To better understand the influence of residue 331 on substrate adaption and to explore the synthetic potential of the already engineered enzyme variants, a series of structurally diverse aromatic aldehydes were subjected to hydrocyanation with the *Pc*HNL5 variants (Table S5, for details see the Supporting Information). The corresponding cyanohydrins of these aldehydes tested are found in scaffolds of pharmaco- or natural product compounds (Figure S115): tranquilizers (**2e**, **2f**),[22] anticonvulsants (**2g**),[23] β-blockers (**2h**, **2j**, **2k**),[24] β_1-adrenergic receptor agonists (**2l**),[25] and ACE-inhibitors (**2p**).[26] Each of these aldehydes was used successfully as a substrate for at least one of the L331 variants with much higher activity than the WT *Pc*HNL5. Substitution of Leu 331 into other hydrophobic residues with a smaller side chain, such as alanine or valine, gave up to 2 orders of magnitude higher activity toward the majority of 3,4-substituted ring-fused aldehydes (**1b**−**1j**) and the more complicated 7-ethyl-benzofuran-2-carbaldehyde (**1k**). Similar phenomena were observed when substrates bearing an alkyl linker with an aromatic ring (**1g**, **1p**) were assayed with the L331 variants, albeit the top hit for **1g** was L331G, which may be due to the larger size of the piperonyl ring when compared with that of **1p**. In contrast, different substitutions at other positions of the benzene ring, such as the 3,5-substituted (**1o**) or 2,3-substituted aryl aldehyde (**1i**), were also accepted by a few L331 variants with a bulky side chain like phenylalanine (L331F) or tryptophan (L331W). Notably, when L331 variants with either a hydrophobic or hydrophilic residue were used to catalyze 4-hydroxy benzaldehyde (**1l**) bearing an electronically withdrawing but less sterically hindered group, only a slight increase in activity was observed. In contrast, L331 variants with smaller hydrophobic residues (e.g., L331 V or L331A) showed a clear increase in enzyme activity toward the bulky 4-phenyl-benzaldehyde (**1m**). These results suggest that the steric effect of the side chain of L331 or its variants interacting with the 2,3,4-substituted benzene ring of substrates, rather than the hydrophobicity, is mainly responsible for the observed difference in enzymatic hydrocyanation reactions.

Performance of the WT enzyme with the best-performing variants in a biphasic hydrocyanation reaction was subsequently compared (Table 2). Most aldehydes were loaded

Table 1. Saturation Kinetic Data of *Pc*HNL5$_{WT}$ and Selected Variants[a]

aldehyde	enzyme	K_m [mM]	k_{cat} [s^{-1}]	K_{cat}/K_m [s^{-1} mM^{-1}]	folds[b]
1a	WT	1.8	137	76	1.0
	L331V	5.4	133	25	0.33
	L331A	28	247	8.8	0.12
	L331G	>30[c]	>40[d]	n.a.[e]	<0.018[f]
1b	WT	37	12	0.32	1.0
	L331V	6.9	26	3.8	13
	L331A	7.6	26	3.4	11
	L331G	13	2.3	0.18	0.57
1c	WT	70	1.0	0.014	1.0
	L331V	11	8.2	0.72	53
	L331A	4.0	17	4.2	297
	L331G	24	13	0.55	39
1d	WT	36	0.026	7.2 × 10^{-4}	1.0
	L331V	14	0.87	0.063	87
	L331A	2.2	4.1	1.8	2526
	L331G	2.2	1.4	0.64	888

[a]The kinetic parameters were determined using substrate concentrations of 0.25−30 mM for **1a**, 0.5−30 mM for **1b**, 0.5−20 mM for **1c**, and 0.5−15 mM for **1d**. See the Supporting Information for details. [b]The folds of k_{cat}/K_m change for the specified variant over the WT enzyme. [c]The K_m value was beyond the maximal concentration due to limited solubility. Thus, it was calculated by an extrapolation method. [d]Calculated from the highest reaction rate determined. [e]Not available in this case. [f]Calculated from the highest k_{cat}/K_m detected.

https://dx.doi.org/10.1021/acscatal.0c01103
ACS Catal. 2020, 10, 5757−5763

Table 2. Asymmetric Hydrocyanation of Structurally Diverse Aryl Aldehydes by *Pc*HNL5$_{WT}$ and Its Variants[a]

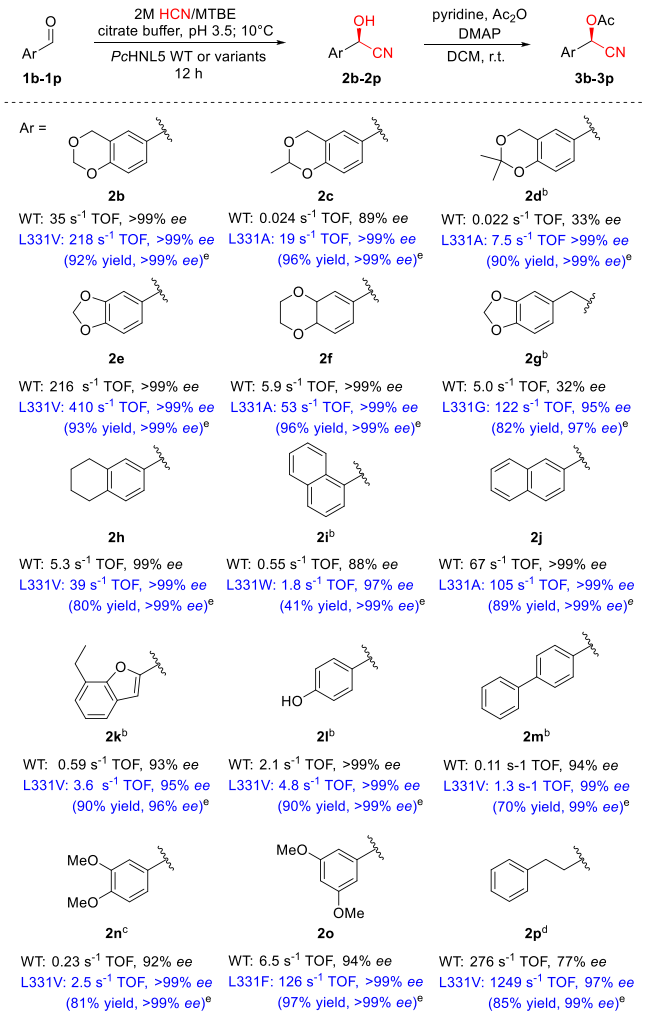

[a]A biphasic reaction mixture (1 mL) was composed of 0.1 mg of purified HNL, 0.3 mL citrate buffer (100 mM, pH 3.5), 0.7 mL of HCN-MTBE (2 M), and varying amounts of aldehydes **1a**−**1p** (**1b**, **1c**, **1f**, **1g**, and **1h**, 0.5 mmol; **1e**, **1j**, **1o**, and **1p**, 1 mmol; **1f**, 0.3 mmol; **1d**, **1i**, **1m**, and **1k**, 0.2 mmol; **1l**, 0.1 mmol; **1n**, 0.05 mmol). Reactions were carried out at 10 °C and 1500 rpm for 12 h. For experimental details of TOF determination, see Supporting Information. [b]0.2 mg of HNL was used. [c]0.3 mg of HNL was used. [d]0.02 mg of HNL was used. [e]The preparative scale reactions were performed using fermentation broths (supernatant portion) of *Pc*HNL5-L331X variants after high cell-density fermentation in a 5-L bioreactor. Isolated yields and ee values were calculated based on *O*-acetylated cyanohydrins obtained after a two-step transformation. See the Supporting Information for details.

over a final concentration range of 0.1−1.0 M with a minimum enzyme dosage of 0.015 wt %. Mutagenesis did not affect the good stability of the L331 variants under acidic conditions, even with increased acid tolerance (Figure S3). This allows the enzymatic hydrocyanation to be performed at low pH to suppress the nonselective chemical HCN addition reaction. Compared with the wild type enzyme, the turnover frequency (TOF or k_{cat}) of the variants improved by 1.6 to 792-fold, even when the substrate was well accepted by WT *Pc*HNL5 (e.g., **1b**, **1e**, **1j**, **1p**). Because asymmetric biohydrocyanation is a competitive process against a spontaneous nonselective addition,[27] the most effective method to mitigate the problem is to employ an enzyme with higher activity or dosage to override the competing reaction.[28] Thus, the L331 variants of *Pc*HNL5 are a set of attractive tools that provide a biocatalytic solution for substrates (e.g., **1g**, **1p**) suffering from severe reactivity of nonenzymatic addition, where both the optical purity and productivity of the cyanohydrin products were clearly improved. Notably, because a high cell-density fermentation of the recombinant *Pichia pastoris* could produce over 1 g L^{-1} of secreted *Pc*HNL5 (Table S6), the direct use of a simple acidized fermentation broth (the supernatant portion) and subsequent acetylation afforded all of the *O*-protected unnatural cyanohydrins (Table 2), including the poorest substrate 1-naphthaldehyde (**1i**), with moderate to satisfying yields (41%−97%) and ideal enantiopurity (96% to >99% ee) within 12 h.

Finally, to demonstrate the practical feasibility of the tailored *Pc*HNL5 variants, we devised the chemo-enzymatic synthesis of (*R*)-salmeterol (Scheme 2), which is a popular long-term β_2-agonist used in the clinic.[29] In a 100 mL biphasic reaction system, 5 g of substrate **1d** was subjected to hydrocyanation by employing only 0.5 wt % of *Pc*HNL5-L331A. The reaction proceeded smoothly to give (*R*)-**2d** in 93% isolated yield and >99% ee within 16 h. A reduction with lithium aluminum hydride in THF gave the corresponding 2-amino-1-alcohol **4** without deterioration of enantiopurity. The subsequent *N*′-alkylation with bromide **5** and deprotection of the isopropylidene group in an aqueous solution of acetic acid afforded (*R*)-salmeterol acetate in an optically pure form (>99% ee). The overall transformation from the readily available aldehyde (**1d**) to the target molecule was realized in four steps with 54% overall yield. This chemo-enzymatic route represents the highest overall yield and optical purity reported for (*R*)-salmeterol. Importantly, these results demonstrate the

Scheme 2. Chemo-Enzymatic Gram-Scale Synthesis of (*R*)-Salmeterol[a]

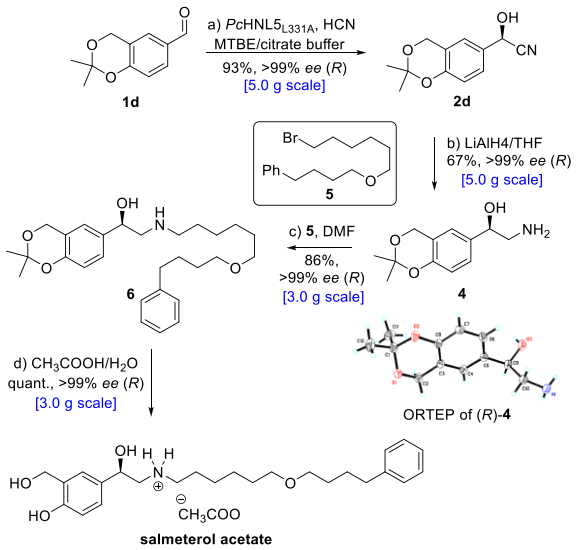

[a]Reaction and conditions: (a) *Pc*HNL5$_{L331A}$ (0.5 wt %), HCN (∼1 M in MTBE, 4 equiv), citrate buffer (100 mM, pH 3.5, 50% v/v), 10 °C, 16 h, 93%; (b) $LiAlH_4$ (1.8 equiv), THF, 0 °C to RT, 8 h. 67% (recrystallization); (c) bromide **5**, DMF, RT, 70 h, 86%; (d) HOAc/water (3/1, v/v), 50 °C, 4 h, quant. MTBE = methyl *tert*-butyl ether; THF = tetrahydrofuran; DMF = *N*,*N*-dimethylformamide.

https://dx.doi.org/10.1021/acscatal.0c01103
ACS Catal. 2020, 10, 5757−5763

great potential of protein engineering for resolving conflicts between the demanding synthetic requirements and the inherent properties of native enzymes in the development of new chemo-enzymatic methods.

In summary, we have successfully engineered a hydroxynitrile lyase that enables asymmetric hydrocyanation of a very challenging rigid benzo-ketal aldehyde. By utilizing the rationally redesigned variants, we were able to realize the first and highly efficient chemo-enzymatic synthesis of an optically pure long-term β_2-agonist via asymmetric C−C bond formation. Furthermore, exploring the substrate spectrum of the engineered enzymes allowed a deeper insight into the crucial role of residue 331 in precisely regulating the substrate acceptability of this enzyme family, thereby providing guidance for future bioconversion of various unnatural aldehydes, especially those with bulky and rigid substitution groups on the aromatic ring. We anticipate that this work will act as a valuable example and lay the foundation for overcoming enzyme limitations in the development of new chemo-enzymatic approaches to atom-economic and eco-friendly syntheses.

■ ASSOCIATED CONTENT

Supporting Information

The Supporting Information is available free of charge at https://pubs.acs.org/doi/10.1021/acscatal.0c01103.

Materials and chemicals; detailed experimental and computational protocols; supporting schemes, tables, and figures for the primers design; expression, purification, and crystallization of *Pc*HNL5; synthetic details; GC and HPLC analytic conditions; GC and HPLC profiles, NMR profiles, and MS profiles; and fermentation details (PDF)

■ AUTHOR INFORMATION

Corresponding Authors

Ran Hong − *CAS Key Laboratory of Synthetic Chemistry of Natural Substances, Center for Excellence in Molecular Synthesis, Shanghai Institute of Organic Chemistry, Chinese Academy of Sciences, Shanghai 200032, China; University of the Chinese Academy of Sciences, Beijing 100049, China;* orcid.org/0000-0002-7602-539X; Email: rhong@sioc.ac.cn

Hui-Lei Yu − *State Key Laboratory of Bioreactor Engineering, Shanghai Collaborative Innovation Centre for Biomanufacturing and Frontiers Science Center for Materiobiology and Dynamic Chemistry, East China University of Science and Technology, Shanghai 200237, China;* Email: huileiyu@ecust.edu.cn

Jian-He Xu − *State Key Laboratory of Bioreactor Engineering, Shanghai Collaborative Innovation Centre for Biomanufacturing and Frontiers Science Center for Materiobiology and Dynamic Chemistry, East China University of Science and Technology, Shanghai 200237, China;* orcid.org/0000-0003-0140-3808; Email: jianhexu@ecust.edu.cn

Authors

Yu-Cong Zheng − *State Key Laboratory of Bioreactor Engineering, Shanghai Collaborative Innovation Centre for Biomanufacturing, East China University of Science and Technology, Shanghai 200237, China*

Fu-Long Li − *State Key Laboratory of Bioreactor Engineering, Shanghai Collaborative Innovation Centre for Biomanufacturing, East China University of Science and Technology, Shanghai 200237, China;* orcid.org/0000-0002-2460-3266

Zuming Lin − *CAS Key Laboratory of Synthetic Chemistry of Natural Substances, Center for Excellence in Molecular Synthesis, Shanghai Institute of Organic Chemistry, Chinese Academy of Sciences, Shanghai 200032, China*

Guo-Qiang Lin − *CAS Key Laboratory of Synthetic Chemistry of Natural Substances, Center for Excellence in Molecular Synthesis, Shanghai Institute of Organic Chemistry, Chinese Academy of Sciences, Shanghai 200032, China; University of the Chinese Academy of Sciences, Beijing 100049, China*

Complete contact information is available at: https://pubs.acs.org/10.1021/acscatal.0c01103

Author Contributions

All authors have given approval to the final version of the manuscript.

Notes

The authors declare no competing financial interest.

■ ACKNOWLEDGMENTS

This work was financially supported by the National Key Research and Development Program of China (Grants 2019YFA09005000 and 2018YFC1706200), the National Natural Science Foundation of China (Grants 21536004, 21922804, 21776085, and 21871085), the Chinese Academy of Sciences (Grants XDB20020000 and QYZDY-SSWSLH026), and the Fundamental Research Funds for the Central Universities (Grant 22221818014). We thank Professor Romas J. Kazlauskas (UMN) for his critical reading and valuable suggestions, Miss Lian Wu (SIOC), and Dr. Guang Liu (ECUST) for their helpful guidance in the addition of NAG during the data refinement of the crystal structure, Dr. Xu-Dong Kong (ECUST), Dr. Fei-Fei Chen (ECUST), and Dr. Qi Chen (ECUST) for their insightful discussions, and Mr. Jun Zhu (ECUST) for his experimental assistance. We are also grateful for the access to beamline BL17U1 and BL19U1 at Shanghai Synchrotron Radiation Facility and thank the beamline staff for the technical help.

■ REFERENCES

(1) Helmchen, G. Introduction: General Concepts. In *Comprehensive Chirality*, Vol. *4: Synthetic Methods III−Catalytic Methods: C−C Bond Formation*; Carreira, E. M., Yamamoto, H., Eds.; Elsevier: Amsterdam, The Netherlands, 2012; p 1.

(2) Corey, E. J.; Kurti, L. *Enantioselective Chemical Synthesis: Methods, Logic and Practice*; Elsevier, 2012; pp 56−120.

(3) (a) Brovetto, M.; Gamenara, D.; Saenz Mendez, P.; Seoane, G. A. C-C Bond-Forming Lyases in Organic Synthesis. *Chem. Rev.* **2011**, *111*, 4346−4403. (b) Hönig, M.; Sondermann, P.; Turner, N. J.; Carreira, E. M. Enantioselective Chemo- and Biocatalysis: Partners in Retrosynthesis. *Angew. Chem., Int. Ed.* **2017**, *56*, 8942−8973.

(4) Turner, N. J.; O'Reilly, E. Biocatalytic retrosynthesis. *Nat. Chem. Biol.* **2013**, *9*, 285−288. (b) Fesko, K.; Gruber-Khadjawi, M. Biocatalytic Methods for C−C Bond Formation. *ChemCatChem* **2013**, *5*, 1248−1272.

(5) (a) Dadashipour, M.; Asano, Y. Hydroxynitrile Lyases: Insights into Biochemistry, Discovery, and Engineering. *ACS Catal.* **2011**, *1*, 1121−1149. (b) Bracco, P.; Busch, H.; von Langermann, J.; Hanefeld, U. Enantioselective Synthesis of Cyanohydrins Catalysed by Hydroxynitrile Lyases − A Review. *Org. Biomol. Chem.* **2016**, *14*,

6375−6389. (c) Purkarthofer, T.; Gruber, K.; Gruber-Khadjawi, M.; Waich, K.; Skranc, W.; Mink, D.; Griengl, H. A Biocatalytic Henry Reaction—The Hydroxynitrile Lyase from *Hevea brasiliensis* Also Catalyzes Nitroaldol Reactions. *Angew. Chem., Int. Ed.* **2006**, *45*, 3454−3456. (d) Bekerle-Bogner, M.; Gruber-Khadjawi, M.; Wiltsche, H.; Wiedner, R.; Schwab, H.; Steiner, K. (*R*)-Selective Nitroaldol Reaction Catalyzed by Metal-Dependent Bacterial Hydroxynitrile Lyases. *ChemCatChem* **2016**, *8*, 2214−2216. (e) Rao, D. H. S.; Padhi, S. K. Production of (S)-β-Nitro Alcohols by Enantioselective C−C Bond Cleavage with an R-Selective Hydroxynitrile Lyase. *ChemBioChem* **2019**, *20*, 371−378.

(6) Gupta, P.; Mahajan, N. Biocatalytic Approaches towards the Stereoselective Synthesis of Vicinal Amino Alcohols. *New J. Chem.* **2018**, *42*, 12296−12327.

(7) (a) Glieder, A.; Weis, R.; Skranc, W.; Poechlauer, P.; Dreveny, I.; Majer, S.; Wubbolts, M.; Schwab, H.; Gruber, K. Comprehensive Step-by-Step Engineering of an (*R*)-Hydroxynitrile Lyase for Large-Scale Asymmetric Synthesis. *Angew. Chem., Int. Ed.* **2003**, *42*, 4815−4818. (b) Bühler, H.; Effenberger, F.; Förster, S.; Roos, J.; Wajant, H. Substrate Specificity of Mutants of the Hydroxynitrile Lyase from *Manihot esculenta*. *ChemBioChem* **2003**, *4*, 211−216. (c) Weis, R.; Gaisberger, R.; Skranc, W.; Gruber, K.; Glieder, A. Carving the Active Site of Almond *R*-HNL for Increased Enantioselectivity. *Angew. Chem., Int. Ed.* **2005**, *44*, 4700−4704. (d) Wiedner, R.; Kothbauer, B.; Pavkov-Keller, T.; Gruber-Khadjawi, M.; Gruber, K.; Schwab, H.; Steiner, K. Improving the Properties of Bacterial *R*-Selective Hydroxynitrile Lyases for Industrial Applications. *ChemCatChem* **2015**, *7*, 325−332.

(8) (a) Holgate, S. T.; Polosa, R. Treatment strategies for allergy and asthma. *Nat. Rev. Immunol.* **2008**, *8*, 218−230. (b) Cazzola, M.; Calzetta, L.; Matera, M. G. β_2-Adrenoceptor Agonists: Current and Future Direction. *Br. J. Pharmacol.* **2011**, *163*, 4−17.

(9) (a) Hett, R.; Stare, R.; Helquist, P. Enantioselective Synthesis of Salmeterol via Asymmetric Borane Reduction. *Tetrahedron Lett.* **1994**, *35*, 9375−9378. (b) Bream, R. N.; Ley, S. V.; McDermott, B.; Procopiou, P. A. A Mild, Enantioselective Synthesis of (*R*)-Salmeterol via Sodium Borohydride−calcium Chloride Asymmetric Reduction of a Phenacyl Phenylglycinol Derivative. *J. Chem. Soc., Perkin Trans.* **2002**, *1*, 2237−2242.

(10) (a) Goswami, J.; Bezbaruah, R. L.; Goswami, A.; Borthakur, N. A Convenient Stereoselective Synthesis of (*R*)-(−)-Denopamine and (*R*)-(−)-Salmeterol. *Tetrahedron: Asymmetry* **2002**, *12*, 3343−3348. (b) Procopiou, P. A.; Morton, G. E.; Todd, M.; Webb, G. Enantioselective Synthesis of (*S*)-Salmeterol via Asymmetric Reduction of Azidoketone by *Pichia angusta*. *Tetrahedron: Asymmetry* **2001**, *12*, 2005−2008.

(11) Liu, J. T.; Zhou, D.; Jia, X.; Huang, L.; Li, X. S.; Chan, A. S. C. A Convenient Synthesis of (*R*)-Salmeterol via Rh-Catalyzed Asymmetric Transfer Hydrogenation. *Tetrahedron: Asymmetry* **2008**, *19*, 1824−1828.

(12) Bream, R. N.; Ley, S. V.; Procopiou, P. A. Synthesis of the β_2 Agonist (*R*)-Salmeterol Using a Sequence of Supported Reagents and Scavenging Agents. *Org. Lett.* **2002**, *4*, 3793−3796.

(13) Buchanan, D. J.; Dixon, D. J.; Looker, B. E. A Short Stereoselective Synthesis of (*R*)-Salmeterol. *Synlett* **2005**, *2005*, 1948−1949.

(14) Guo, Z. L.; Deng, Y. Q.; Zhong, S.; Lu, G. Enantioselective Synthesis of (*R*)-Salmeterol Employing an Asymmetric Henry Reaction as the Key Step. *Tetrahedron: Asymmetry* **2011**, *22*, 1395−1399.

(15) Effenberger, F.; Jäger, J. Synthesis of the Adrenergic Bronchodilators (*R*)-Terbutaline and (*R*)-Salbutamol from (*R*)-Cyanohydrins. *J. Org. Chem.* **1997**, *62*, 3867−3873.

(16) Caira, M. R.; Hunter, R.; Nassimbeni, L. R.; Stevens, A. T. Resolution of Albuterol Acetonide. *Tetrahedron: Asymmetry* **1999**, *10*, 2175−2189.

(17) Zheng, Y. C.; Xu, J. H.; Wang, H.; Lin, G. Q.; Hong, R.; Yu, H. L. Hydroxynitrile Lyase Isozymes from *Prunus communis*: Identification, Characterization and Synthetic Applications. *Adv. Synth. Catal.* **2017**, *359*, 1185−1193.

(18) (a) Arnold, F. H. Directed Evolution: Bringing New Chemistry to Life. *Angew. Chem., Int. Ed.* **2018**, *57*, 4143−4148. (b) Xu, F.; Kosjek, B.; Cabirol, F. L.; Chen, H. B.; Desmond, R.; Park, J.; Gohel, A. P.; Collier, S. J.; Smith, D. J.; Liu, Z. Q.; Janey, J. M.; Chung, J. Y. L.; Alvizo, O. Synthesis of Vibegron Enabled by a Ketoreductase Rationally designed for high pH DKR. *Angew. Chem., Int. Ed.* **2018**, *57*, 6863−6867. (c) Chen, F. F.; Cosgrove, S. C.; Birmingham, W. R.; Mangas-Sanchez, J.; Citoler, J.; Thompson, M. P.; Zheng, G. W.; Xu, J. H.; Turner, N. J. Enantioselective Synthesis of Chiral Vicinal Amino Alcohols Using Amine Dehydrogenases. *ACS Catal.* **2019**, *9*, 11813−11818. (d) Huffman, M. A.; Fryszkowska, A.; Alvizo, O.; Borra-Garske, M.; Campos, K. R.; Canada, K. A.; Devine, P. N.; Duan, D.; Forstater, J. H.; Grosser, S. T.; Halsey, H. M.; Hughes, G. J.; Jo, J.; Joyce, L. A.; Kolev, J. N.; Liang, J.; Maloney, K. M.; Mann, B. F.; Marshall, N. M.; McLaughlin, M.; Moore, J. C.; Murphy, G. S.; Nawrat, C. C.; Nazor, J.; Novick, S.; Patel, N. R.; Rodriguez-Granillo, A.; Robaire, S. A.; Sherer, E. C.; Truppo, M. D.; Whittaker, A. M.; Verma, D.; Xiao, L.; Xu, Y.; Yang, H. Design of An In Vitro Biocatalytic Cascade for the Manufacture of Islatravir. *Science* **2019**, *366*, 1255−1259.

(19) (a) Dreveny, I.; Andryushkova, A. S.; Glieder, A.; Gruber, K.; Kratky, C. Substrate Binding in the FAD-Dependent Hydroxynitrile Lyase from Almond Provides Insight into the Mechanism of Cyanohydrin Formation and Explains the Absence of Dehydrogenation Activity. *Biochemistry* **2009**, *48*, 3370−3377. (b) Pavkov-Keller, T.; Bakhuis, J.; Steinkellner, G.; Jolink, F.; Keijmel, E.; Birner-Gruenberger, R.; Gruber, K. Structures of Almond Hydroxynitrile Lyase Isoenzyme 5 Provide A Rationale for the Lack of Oxidoreductase Activity in Flavin Dependent HNLs. *J. Biotechnol.* **2016**, *235*, 24−31.

(20) Chovancova, E.; Pavelka, A.; Benes, P.; Strnad, O.; Brezovsky, J.; Kozlikova, B.; Gora, A.; Sustr, V.; Klvana, M.; Medek, P.; Biedermannova, L.; Sochor, J.; Damborsky, J. CAVER 3.0: A Tool for the Analysis of Transport Pathways in Dynamic Protein Structures. *PLoS Comput. Biol.* **2012**, *8*, No. e1002708.

(21) (a) Sun, Z. T.; Lonsdale, R.; Wu, L.; Li, G. Y.; Li, A. T.; Wang, J. B.; Zhou, J.; Reetz, M. T. Structure-Guided Triple-Code Saturation Mutagenesis: Efficient Tuning of the Stereoselectivity of an Epoxide Hydrolase. *ACS Catal.* **2016**, *6*, 1590−1597. (b) Sun, Z. T.; Salas, P. T.; Siirola, E.; Lonsdale, R.; Reetz, M. T. Exploring Productive Sequence Space in Directed Evolution using Binary Patterning versus Conventional Mutagenesis Strategies. *Bioresour. Bioprocess.* **2016**, *3*, 44. (c) Sun, Z. T.; Lonsdale, R.; Li, G. Y.; Reetz, M. T. Comparing Different Strategies in Directed Evolution of Enzyme Stereoselectivity: Single- versus Double-Code Saturation Mutagenesis. *ChemBioChem* **2016**, *17*, 1865−1872. (d) Li, F. L.; Kong, X. D.; Chen, Q.; Zheng, Y. C.; Xu, Q.; Chen, F. F.; Fan, L. Q.; Lin, G. Q.; Zhou, J.; Yu, H. L.; Xu, J. H. Regioselectivity Engineering of Epoxide Hydrolase: Near-Perfect Enantioconvergence through a Single Site Mutation. *ACS Catal.* **2018**, *8*, 8314−8317. (e) Qu, G.; Lonsdale, R.; Yao, P. Y.; Li, G. Y.; Liu, B. B.; Reetz, M. T.; Sun, Z. T. Methodology Development in Directed Evolution: Exploring Options when Applying Triple-Code Saturation Mutagenesis. *ChemBioChem* **2018**, *19*, 239−246.

(22) Effenberger, F.; Jäger, J. Stereoselective Synthesis of (*S*)-3,4 Methylenedioxyamphetamines from (*R*)-Cyanohydrins. *Chem. - Eur. J.* **1997**, *3*, 1370−1374.

(23) Anderson, B. A.; Hansen, M. M.; Varie, D. L.; Vicenzi, J. T.; Zeijewski, M. J. *Stereoselective Process for Producing Dihydro-2,3-benzodiazepine Derivatives*. EP 0699677, 1999.

(24) (a) Howe, R.; Rao, B. S. β-Adrenergic Blocking Agents. III. The Optical Isomers of Pronethalol, Propranolol, and Several Related Compounds. *J. Med. Chem.* **1968**, *11*, 1118−1121. (b) Chen, W.; Zhou, Z. H.; Chen, H. B. Efficient Synthesis of Chiral Benzofuryl β-Amino Alcohols via A Catalytic Asymmetric Henry Reaction. *Org. Biomol. Chem.* **2017**, *15*, 1530−1536. (c) Jackson, W. R.; Jacobs, H. A.; Jayatilake, G. S.; Matthews, B. R.; Watson, K. G. Applications of

Optically Active Aryl Cyanohydrins in the Synthesis of α-Hydroxy Aldehydes, α-Hydroxy Ketones and β-Hydroxy Amines. *Aust. J. Chem.* **1990**, *43*, 2045−2062.

(25) Brown, R. F. C.; Donohue, A. C.; Jackson, W. R.; McCarthy, T. D. Synthetic Applications of Optically Active Cyanohydrins. Enantioselective Syntheses of the Hydroxyamides Tembamide and Aegeline, the Cardiac Drug Denopamine, and Some Analogues of the Bronchodilator Salbutamol. *Tetrahedron* **1994**, *50*, 13739−13752.

(26) (a) Lima, D. P.; Quim, D. Synthesis of Angiotensin-Converting Enzyme (ACE) Inhibitors: An Important Class of Antihypertensive Drugs. *Quim. Nova* **1999**, *22*, 375−381. (b) Tikare, R. K. *Synthesis of Chiral Intermediates Useful in Preparing Pharmacologically Active Compounds*. WO 0242244A, 2004.

(27) Andexer, J. N.; Langermann, J. V.; Kragl, U.; Pohl, M. How to Overcome Limitations in Biotechnological Processes − Examples from Hydroxynitrile Lyase Applications. *Trends Biotechnol.* **2009**, *27*, 599−607.

(28) (a) Hanefeld, U. Immobilisation of Hydroxynitrile Lyases. *Chem. Soc. Rev.* **2013**, *42*, 6308−6321. (b) Dadashipour, M.; Ishida, Y.; Yamamoto, K.; Asano, Y. Discovery and Molecular and Biocatalytic Properties of Hydroxynitrile Lyase from An Invasive Millipede, Chamberlinius hualienensis. *Proc. Natl. Acad. Sci. U. S. A.* **2015**, *112*, 10605−10610.

(29) Cazzola, M.; Donner, C. F. Long-acting β_2 Agonists in the Management of Stable Chronic Obstructive Pulmonary Disease. *Drugs* **2000**, *60*, 307−320.

https://dx.doi.org/10.1021/acscatal.0c01103
ACS Catal. 2020, 10, 5757−5763